16 Lecture 16. General picture of Hamiltonian systems

16.1 Completely integrable systems

We know the Liouville-Arnold theorem (**11.6**): if a system is completely integrable, we have a canonical transformation converting it to a system described by the action-angle variables that parameterize ‘orderly’ trajectories on T^n.
Example: the Toda system: three point masses interacting with the Toda potential (**12.3**)[159],

$$H = \frac{1}{2}(p_x^2 + p_y^2) + \frac{1}{24}\left[\exp(2y + 2\sqrt{3}x) + \exp(27 - 2\sqrt{3}x) + \exp(-4y)\right] - \frac{1}{8}. \quad (16.1)$$

We know how to convert this into the Lax pair representation All the trajectories are periodic or almost periodic (see Fig. 16.1[160]).

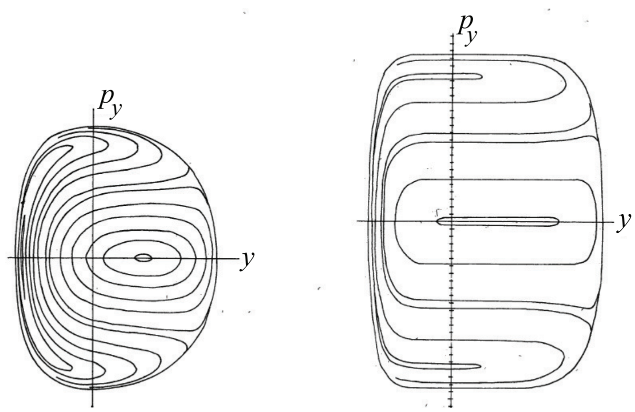

Figure 16.1: Left: A surface of section for the Toda Hamiltonian (16.1) at energy $E = l$. The scales on both axes are the same. The outermost oval crosses the positive p_y-axis at 1.3 and the positive y-axis at 1.4; Right: At energy $E = 256$. Here the scales on two axes are not the same. The outermost oval crosses the positive y-axis at $y = 4$ and the positive p_y-axis at $p_y = 22.6$. All the allowed phase space is surveyed in these figures, because outside the outermost curves $p_x^2 < 0$. [Fig. 1,2 of FORD et al., PTP 50 1547 (1973)]

---

[159] Its polynomial expansion truncated at the third order (the Henon system) is not integrable.

[160] Joseph FORD, Spotswood D. STODDARD and Jack S. Turner, “On the Integrability of the Toda Lattice,” Prog Theor Phys 50 1547 (1973).

16.2 Near integrable systems

The Henon system is obtained by expanding and truncating the Toda Hamiltonian (16.1) as

$$H = \frac{1}{2}(p_x^2 + p_y^2) + \frac{1}{2}(x^2 + y^2) + x^2 y - \frac{1}{3}y^3. \tag{16.2}$$

This describes a motion in the potential that is something like a symmetric monkey saddle. A perturbative approach dissects H into H_0 and H_1 as

$$H_0 = \frac{1}{2}(p_x^2 + p_y^2) + \frac{1}{2}(x^2 + y^2), \tag{16.3}$$

$$\varepsilon H_1 = = \varepsilon\left(x^2 y - \frac{1}{3}y^3\right). \tag{16.4}$$

Comparison between the formal perturbation series (truncated at third order) and numerical results is in Fig. 16.2.[161]

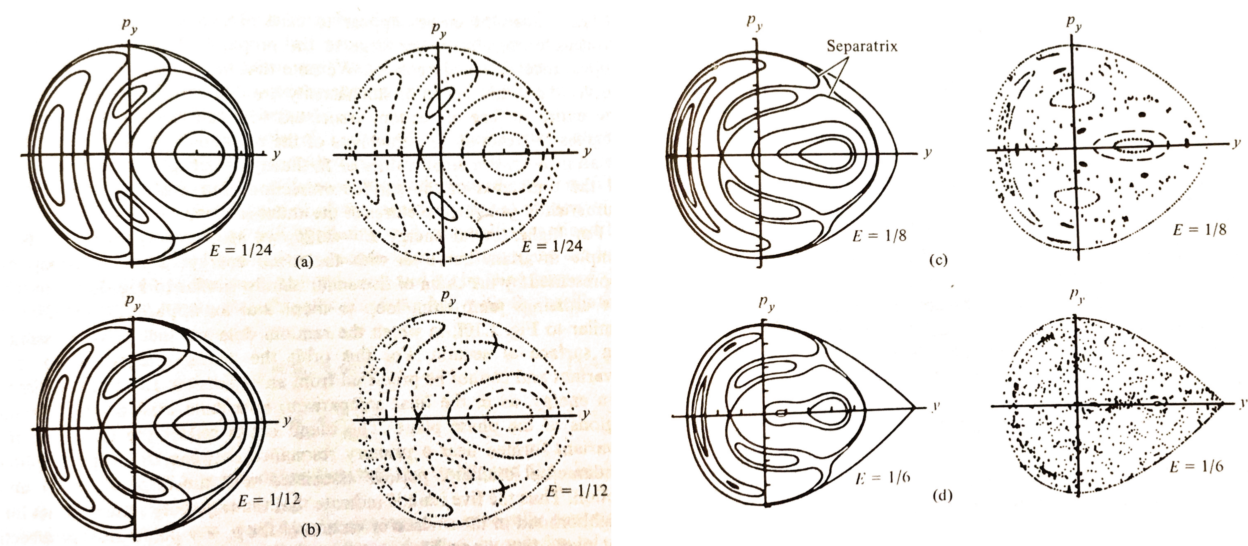

Figure 16.2: Perturbation fails even for small nonintegrable perturbation: [Figs originally from Gustavson Ast J 71 670 (1966).]

The comparison tells us that perturbation series fail to converge.

[161] F. G. Gustavson "On Constructing Formal Integrals of a Hamiltonian System Near an Equilibrium Point," Astronom. J 71 670 (1966). Here, the figure is from A J Lichtenberg andL A Lieberman, *Regular and Stochastic motion* (Springer, Applied Mathematical Science 38, 1983). Fig. 1.13.

16.3 What Poincaré realized when perturbation changes systems qualitatively

The picture Poincaré conceived may look like Fig. 16.3.

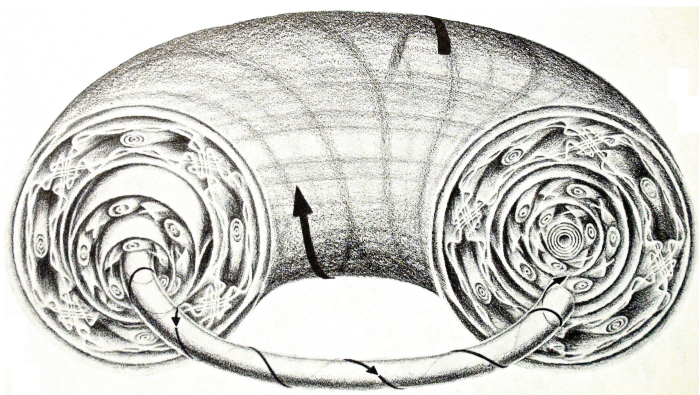

Figure 16.3: What Poincaré conceived (after Arnold) [Fig. 8.3.3 of]

"On January 21, 1889, King Oscar II turned 60. On the same day, the king announced the winner of the mathematics prize that had been established in his name. All treatises had been submitted anonymously, supplied with a title and an envelope containing the author's name, The envelops were now opened with great ceremony. The winner was Henri Poincaré." (p377[162])

"Poincaré's treatise was a comprehensive attempt to answer the question: "Is te solar system stable?" "(p378) However, he discussed the restricted three-body problem. "Mittag-Leffler had informed Hermite that he and Weierstrass thought Poincaré should be awarded the prize... Hermite, who had received copies of the various submissions, agreed. But even though they could immediately see and acknowledge the quality of Poincaré's work, not everything was equally easy to understand. Weierstrass had sought clarification on several points, and Poincaré had sent several extensive addenda. Hermite remarked that, as usual, it was difficult to understand Poincaré—that it was his style to spring over details and leave the reader to fill in the gaps. $\cdots$ According to Hermite, Poincaré was a seer to whom the truth revealed itself in a brilliant light.

Mittag-Leffler's plan was to present the winning submissions in *Acta*[163] in October 1889,

[162] A. Stubhaug, *Gösta Mittag-Leffler, a man of conviction* (translated by Tiina Nunnally, Springer 2010; Norwegian original 2007).

[163] Acts Mathematica

and Phragmén, who acted as the editorial secretary, was handed the big job of editing the treatise. When printing began in July, Phragmén discover several passages in Poincaré's work that seemed quite obscure. Mittag-Leffler immediately pointed this out in a letter to Poincaré, who upon further study found that in another place in the treatise he had made more serious errors. But Poincaré did not report this to Mittag-Leffler until December, and by that time fifty copies of *Acta* had already been printed. These were sent out to subscribers and booksellers, mostly in the Nordic countries, but also to England, France, and Germany. Mittag-Leffler feared that the error would prove ruinous for the reputation of both Poincaré and the journal, as well as Oscar II's entire involvement. He immediately sent a letter to all of these subscribers and booksellers, asking them to return the copies they had received. He explained that certain corrections were necessary." (p379)

Mittag-Leffler "asked Poincaré to pay for the already printed treatise. Poincaré agreed without protest, and his total cost for the new printing was eventually calculated to be 3,500 kronor—1,000 kronor more than the prize money he had received." (p380)

"Poincaré's work totaled 270 pages—the note and addenda filled 93 pages. What was new and brilliant about Poincaré's work eventually overshadowed any talk of errors or corrections." (p380).

16.4 Resonance vs nonresonance

The following example is related to heating ions in confined plasmas (Fig. 16.4).[164] A constant magnetic field and a perpendicularly propagating electrostatic wave with frequency several times the ion cyclotron frequency are applied to charged particles.

Consider a single ion with mass m and charge q in the fields

$$\boldsymbol{B} = B_0\boldsymbol{e}_z, \ \ \boldsymbol{E} = E_0\boldsymbol{e}_y\cos(ky-\omega t). \tag{16.5}$$

These fields are given by the potentials

$$\boldsymbol{A} = -B_0 y\boldsymbol{e}_x, \ \phi = -(E_0/k)\sin(ky-\omega t); \tag{16.6}$$

thus the Hamiltonian H is given by

$$H = \frac{1}{2m}[(p_x+qB_0y)^2+p_y^2] - \frac{qE_0}{k}\sin(ky-\omega t). \tag{16.7}$$

[164]Original: C F F Karney Princeton thesis: Stochastic Ion Heating By a Lower Hybrid Wave (1978). See C F F Kerney and A Ber, Stochastic Ion Heating by a Perpendicularly Propagating Electrostatic Wave, PRL **39**, 550 (1977): "The motion of an ion in the presence of a constant magnetic field and a perpendicularly propagating electrostatic wave with frequency several times the ion cyclotron frequency is shown to become stochastic for fields satisfying ...". The exposition here follows C. F. F. Karey, "Stochastic ion heating by a lower hybrid wave" Phys. Fluid **21**, 1584 (1978).

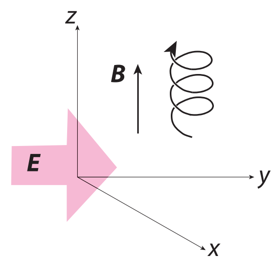

Figure 16.4:

Scaling variables appropriately,[165] the Hamiltonian reads

$$H = \frac{1}{2}[(p_x + y)^2 + p_y^2] - \alpha \sin(y - vt), \tag{16.8}$$

where $v = \omega/\Omega$ and $\alpha = qkE_0/m\Omega^2 = (E_0/B_0)/(\Omega/k)$.

Next, we wish to remove the time dependence. The canonical transformation with the following generator for $(x, p) \to (X, P)$

$$G = (P_x - vt)x + P_y(y - vt + Px) \tag{16.9}$$

would do this:

$$X = x + p_y,\ P_x = p_x + vt,\ Y = y + p_x,\ P_y = p_y, \tag{16.10}$$

and the new Hamiltonian K is given by

$$K = H - vX + \frac{1}{2}(Y^2 + P_y^2) - vX - \alpha \sin(Y - P_x). \tag{16.11}$$

Note that $Y - y$ is a constant of motion p_x, since (16.8) does not depend on x. From (16.8) $\dot{x} = p_x + y$ and p_x is invariant, so we may set $\dot{x} = y$.

Finally, we introduce the action-angle variables through the following generating function

$$F = \frac{1}{2}Y^2 \cot \phi_1 + X\phi_2. \tag{16.12}$$

Thus, (cf **11.9**)

$$P_x = \frac{\partial F}{\partial X},\ P_y = \frac{\partial F}{\partial Y},\ I_1 = -\frac{\partial F}{\partial \phi_1},\ I_2 = -\frac{\partial F}{\partial \phi_2} \tag{16.13}$$

[165] $t \to \Omega t, x \to kx, p \to pk/m\Omega$, where $\Omega = qB_0/m$.

or

$$P_x = \phi_2,\ P_y = Y \cot\phi_1,\ I_1 = Y^2/\sin^2\phi_1,\ I_2 = -X. \tag{16.14}$$

Thus, we get

$$P_x = \phi_2,\ X = -I_2,\ P_y = (2I_1)^{1/2}\cos\phi_1,\ Y = (2I_1)^{1/2}\sin\phi_1. \tag{16.15}$$

The Hamiltonian reads

$$K = I_1 + vI_2 - \alpha\sin[(2I_1)^{1/2}\sin\phi_1 - \phi_2]. \tag{16.16}$$

Depending on the amplitude of the perturbation α, we see what can happen in Fig. 16.5.

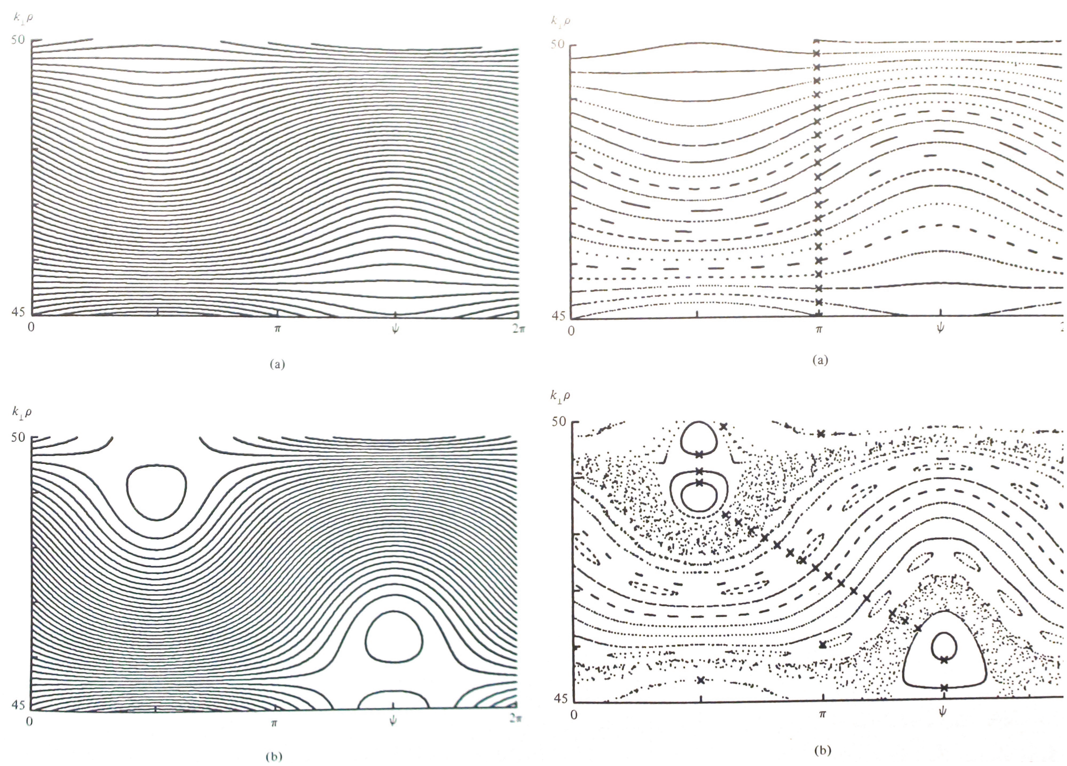

Figure 16.5: [Fig. 2.4, 2.5 of LL p83,4; originals from Karney's thesis]

As can be seen from the figure, if there is no resonance or near resonance in the system analytic results are reliable, but the analytically obtained invariant curves are actually non-existence globally. This causes the ions to heat up.

16.5 Hamiltonian systems and area preserving maps

The Poincaré map of a Hamiltonian system is area preserving. This is due to the invariance of the integral of PdQ under a canonical transformation (see **13.11**), esp., under dynamics. Therefore, it is highly interesting to study an area preserving map from $\mathbb{R}^2$ into itself.

16.6 Twist map

If the system is integrable, the trajectories are on T^2, so the map reads

$$\theta_{n+1} = \theta_n + 2\pi\alpha(J), \tag{16.17}$$

where J is the action variable specifying a torus (integral of motion). The map generally twists the cross section because of $\alpha(J)$.

16.7 General observation about perturbation results

The twist map need not be in terms of J and θ. We can use the usual xy-coordinates as

$$x_{n+1} = x_n \cos\psi - y_n \sin\psi, \tag{16.18}$$

$$y_{n+1} = x_n \sin\psi + y_n \cos\psi, \tag{16.19}$$

where $\psi = 2\pi\alpha$, α being the rotation number. If $\alpha = r/s$, where $r, s \in \mathbb{N}$ and r and s are mutually incongruent, then any point on the circle $\alpha(J) = r/s$ is on a periodic orbit with period s.

If α is irrational, then the circle is filled with a dense orbit.

The KAM-type theorem tells us that the orbits with the rotation number 'irrational enough' survive, but rational orbits are destroyed.

16.8 Poincaré-Birkhoff's theorem

If, in **16.7**, $\alpha = r/s$, after perturbation, most point on the circle is no more periodic, but there still remain even multiple of s fixed points (that is, the s-periodic orbit bifurcates into a period $2ns$ for some $n \in \mathbb{N}^+$) orbit (See Fig. 16.6).

[Demo] We assume the original unperturbed circle is bounded from inside and from outside by KAM curves (surfaces). Between these two KAM curves lies the rational circle for $\alpha = r/s$. This curve is deformed by perturbation, but after s iterations the angular coordinate is unchanged, so it can deform in the radial direction. However, the map is area preserving (**16.5**), so the deformed curve must have even crossings with the unperturbed circle.

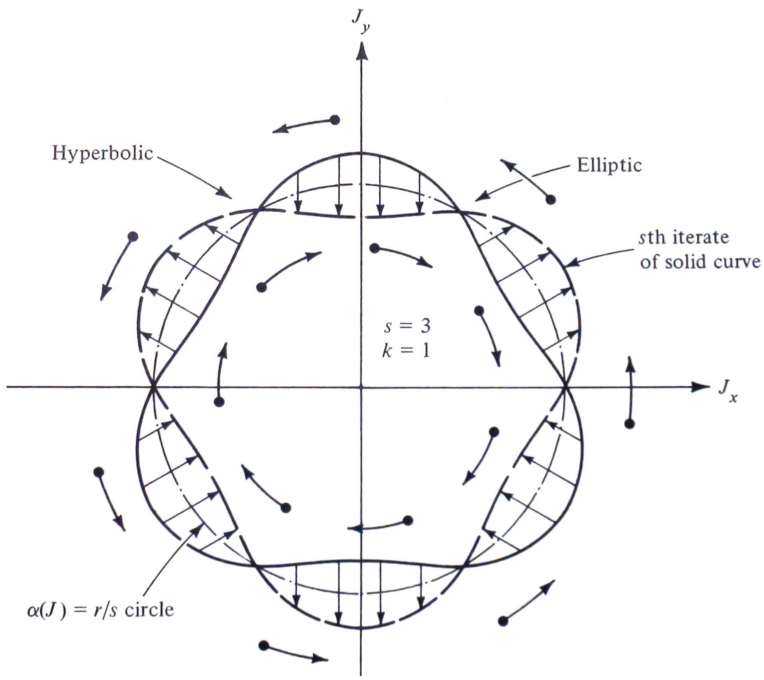

Figure 16.6: For the case $s = 3$ six (6) fixed points could exist after perturbation. [Fig. 3.3 of LL p169]

16.9 Newly formed elliptic and hyperbolic fixed points

As can be seen from Fig. 16.6, a multiple of s of new hyperbolic and elliptic fixed points are formed.

We have ns chain of hyperbolic fixed points. If integrable, we have heteroclinic orbits connecting them, and the remaining orbits are just 'laminar.' as we see for harmonic oscillators.

However, generally, we cannot avoid heteroclinic crossing, causing horseshoes as illustrated in Fig. 16.7.

An actual illustration is furnished by Henon's quadratic twist map:

$$x_{n+1} = x_n \cos\psi - (y_n - x_n^2)\sin\psi, \tag{16.20}$$

$$y_{n+1} = x_n \sin\psi + (y_n - x_n^2)\cos\psi. \tag{16.21}$$

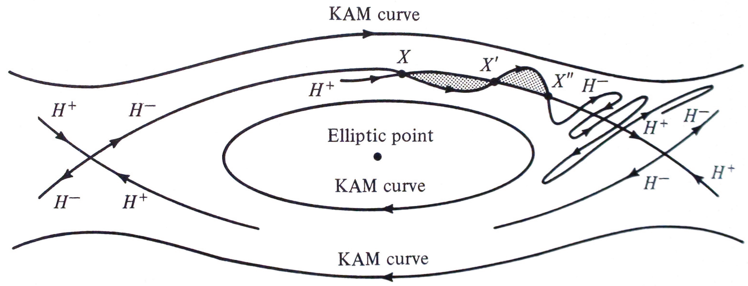

Figure 16.7: Generally we cannot avoid heteroclinic orbits, leading to horseshoe dynamics. [Fig. 3.4a of LL p171]

In Fig. 16.8 $\psi = 2\pi\alpha$ with $\alpha = 0.2114$. The first island or heteroclinic chain is exhibited.

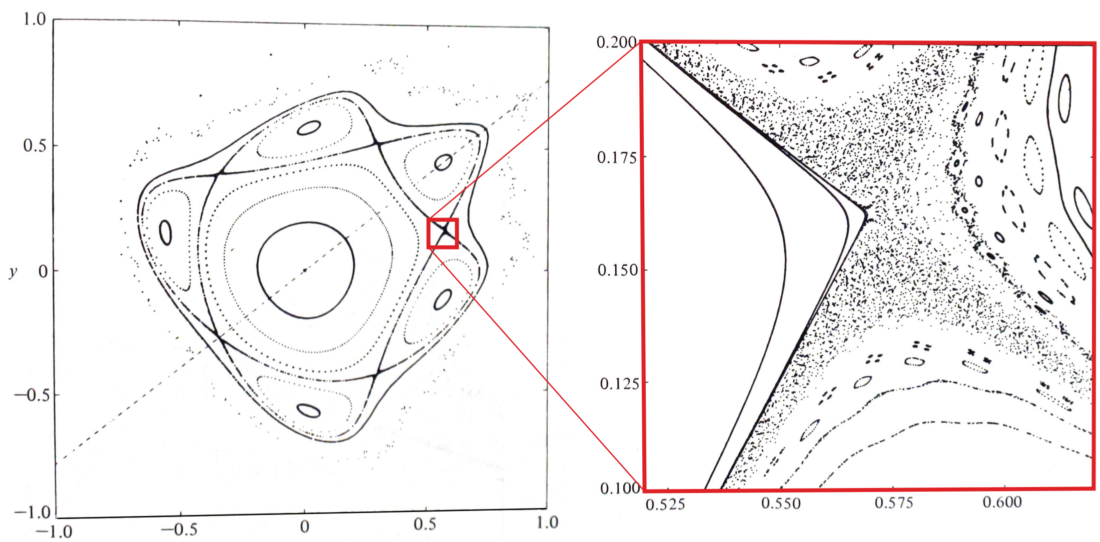

Figure 16.8: Henon quadratic twist map [Fig. 3.6 of LL]

16.10 Standard map or Chirikov-Taylor map

If a completely integrable system is perturbed as

$$H(J, \theta) = H_0(J) + \varepsilon H_1(J, \theta). \tag{16.22}$$

The Poincaré map corresponding to (16.17) must have the following form:

$$J_{n+1} = J_n + \varepsilon f(J_n, \theta_n), \tag{16.23}$$

$$\theta_{n+1} = \theta_n + 2\pi\alpha(J_n) + \varepsilon g(J_n, \theta_n). \tag{16.24}$$

For many interesting cases f does not depend of J and g may be ignored, if J_n in α is replaced by J_{n+1}:

$$J_{n+1} = J_n + \varepsilon f(\theta_n), \tag{16.25}$$
$$\theta_{n+1} = \theta_n + 2\pi\alpha(J_{n+1}). \tag{16.26}$$

Introducing $2\pi\alpha(J) = I$, assuming that the torus does not warp too much and then expanding $2\pi\alpha(J_n + \varepsilon f)$ around $\varepsilon = 0$, ignoring the J dependence of the derivative, we have a linearized equation:

$$I_{n+1} = I_n + Kf(\theta_n), \tag{16.27}$$
$$\theta_{n+1} = \theta_n + I_{n+1}, \tag{16.28}$$

where K is called the stochastic parameter. If we assume further $f(\theta) = \sin\theta$, we get the standard map (or the Chrikov-Taylor[166] map)

$$I_{n+1} = I_n + K\sin\theta_n, \tag{16.29}$$
$$\theta_{n+1} = \theta_n + I_{n+1}, \tag{16.30}$$

This may be interpreted as a simplified model of particle accelerator by a localized oscillating electric field.[167]

K dependence overview:
https://www.youtube.com/watch?v=PgBzZ6CcyPY

16.11 Fermi acceleration problem

The problem of a ball bouncing between a fixed and an oscillating wall is called the Fermi acceleration problem (Fog. 16.9L), because it was first examined by Fermi as a possible mechanism of accelerating cosmic ray particles.

The original moving wall problem can be solved completely, but the problem can be simplified without spoiling its essence by assuming that the wall does not move but

[166] Chirikov (see Phys. Rep. 50 263 (1979)) and Greene used this from to stud the transition to chaos.

[167] $K = (\sqrt{5} - 1)/2$ gives the last KAM surface.

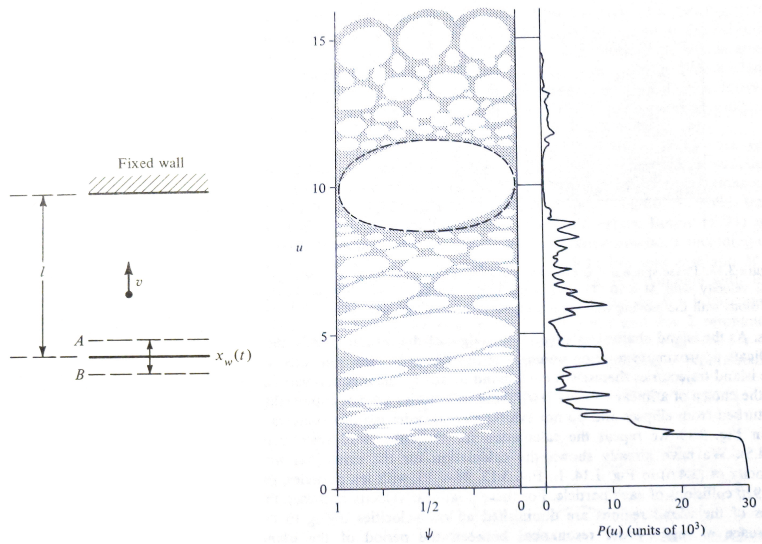

Figure 16.9: Left: Fermi acceleration problem; Right: Phase space (ψ, u) and velocity distribution $P(u)$. $M = 10$ in (16.32) with 7 typical initial conditions. The broken ellipse is the result of secular perturbation theory. [Fig. 3.11a, 3.12 of LL]

somehow gives a kick to the ball. The successive normalized ball speed u_n and the wall phase ψ_n (Sawtooth-like oscillation assumed) obey

$$u_{n+1} = |u_n + \psi_n - 0.5|. \tag{16.31}$$

$$\psi_{n+1} = \psi_n + M/u_n \pmod 1). \tag{16.32}$$

where $M = l/16a$ and $u = MTv/2l$, where l is the wall space, a the oscillation amplitude, T the wall oscillation period in the original problem before simplification. The absolute sign corresponds to the velocity reversal due to reflection. The phase portrait is in Fig. 16.9R.[168]

Saw-tooth standard map:

http://demonstrations.wolfram.com/TheSawtoothStandardMap/

16.12 Fermi problem and standard map

If the wall moves sinusoidally, then (16.32) now becomes the following form (the period of the wall is now scaled to 2π)

$$u_{n+1} = |u_n + \sin\psi_n|, \tag{16.33}$$

[168] M A Lieberman and A J Lichtenberg, Stochastic and adiabatic behavior of particles accelerated by periodic forces, Phys Rev A 5 1872 (1978).

$$\psi_{n+1} = \psi_n + 2\pi M/u_n. \tag{16.34}$$

Then, we linearize the above equation near the fixed point. Such a fixed point is given by $2\pi M/u_1$ being 2π times positive integers. Introduce $\Delta u_n = u_n - u_1$. The second equation of (16.34) becomes

$$\psi_{n+1} = \psi_n + \frac{2\pi M}{u_1} - \frac{2\pi M}{u_1^2}\Delta u_n. \tag{16.35}$$

Here, $2\pi M/u_1$ may be ignored. $\theta_n = \psi_n - \pi$ is used to rewrite the equations as

$$\Delta u_{n+1} = \Delta u_n - \sin\theta_n, \tag{16.36}$$

$$\theta_{n+1} = \theta_n - \frac{2\pi M}{u_1^2}\Delta u_n. \tag{16.37}$$

Then, introduce $I_n = -2\pi M \Delta u_n/u_1^2$, and setting $K = 2\pi M/u_1^2$, we have arrived at the standard map:

$$I_{n+1} = I_n + K\sin\theta_n, \tag{16.38}$$

$$\theta_{n+1} = \theta_n + I_n. \tag{16.39}$$

As can be seen from the derivation, the standard map with various K can mimic the original system around various fixed points as illustrated in Fig. 16.10:

16.13 Arnold diffusion

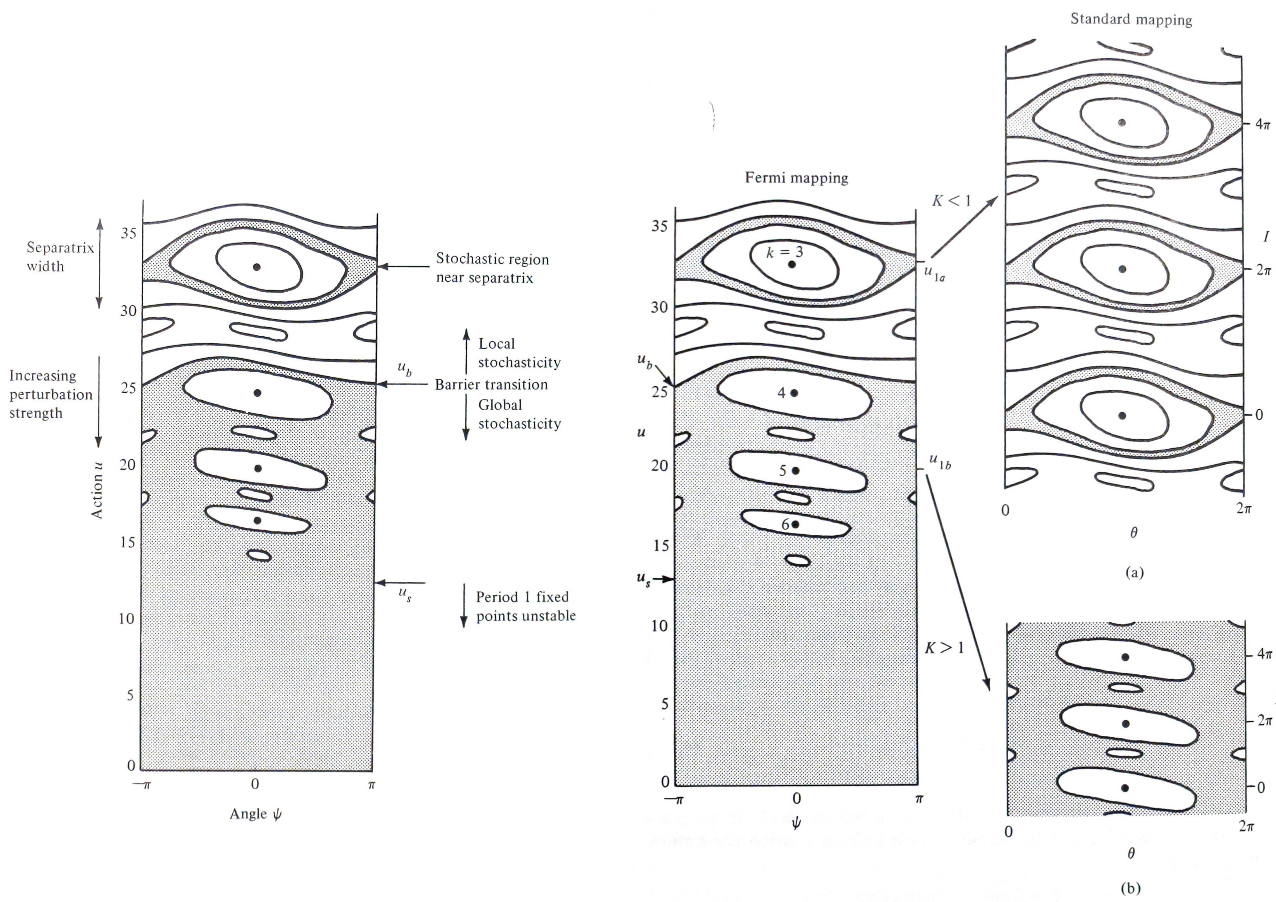

Figure 16.10: Fermi model-standard map correspondence [Fig. 4,1, 2 of LL]

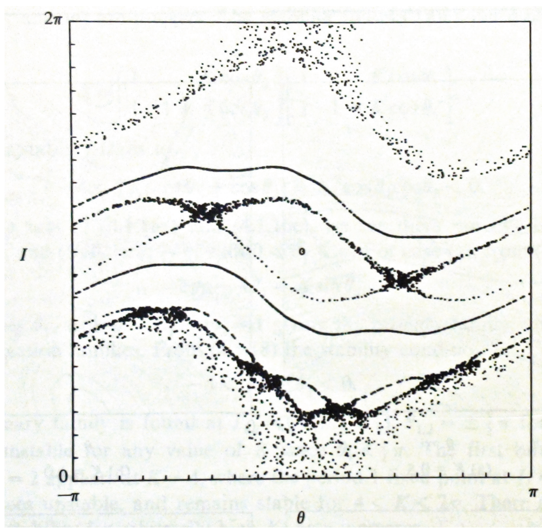

Figure 16.11: Arnold diffusion can be seen away from the fixed point [Fig. 4.4 of LL]